Visual understanding of the hidden-order transition in URu_2Si_2 by high-resolution x-ray Compton scattering

Akihisa Koizumi,[1,*] Yasunori Kubo,[2] Gaku Motoyama,[3] Tomoo Yamamura,[4] Masayoshi Itou,[5] and Yoshiharu Sakurai[5]

[1]*Graduate School of Material Science, University of Hyogo, Hyogo 678-1297, Japan*

[2]*Department of Physics, College of Humanities and Science, Nihon University, Tokyo 156-8550, Japan*

[3]*Department of Physics and Materials Science, Shimane University, Shimane 690-8504, Japan*

[4]*Institute for Materials Research, Tohoku University, Sendai 980-8577, Japan*

[5]*Japan Synchrotron Radiation Research Institute (JASRI), SPring-8, Hyogo 679-5198, Japan*

(Received 6 November 2014; published 8 September 2015)

We report the change of electronic structure associated with the hidden-order (HO) transition in URu_2Si_2 through Compton scattering experiment on the (001) plane of the single crystal. The two-dimensional electron occupation number densities (EONDs) obtained at 14 and 20 K, which are the projection of Fermi volume onto the k_x-k_y plane of the first Brillouin zone, clearly reflect a whole image of electronic structure in the HO and paramagnetic (PM) phases, respectively. The change in electronic structure is well described by theoretical EONDs derived from the result of a band calculation, where U $5f$ electrons are treated as itinerant ones. We also evaluate the electron (hole) numbers in the HO and PM phases and, therefore, its change on the HO transition. The HO transition is deeply involved with a significant change in $5f$ electrons from partially localized to itinerant states through hybridization with conduction electrons, resulting in the reconstruction of Fermi-surface structure.

DOI: 10.1103/PhysRevB.92.125112 PACS number(s): 71.18.+y, 74.25.Jb, 78.70.Ck

I. INTRODUCTION

The hidden-order (HO) transition observed in a heavy fermion compound URu_2Si_2 at $T_{HO} = 17.5$ K has been a matter of concern for the field of a strongly correlated electron system. Despite experimental and theoretical efforts for more than a quarter century, the HO problem is not fully resolved. From a viewpoint of bulk measurement, a sharp jump observed in specific heat at T_{HO}, for instance, is a clear sign of the second-order phase transition; hence, a significant fraction of total entropy should be removed [1–3]. However, the order parameter of the HO phase is still unidentified by way of experiment. Several theories have recently proposed novel ideas, such as modulated spin liquid, spin nematic order, rank-5 nematic order, and hastatic order [4–7]. These theories account for the HO transition and therefore would be likely scenarios, although it seems difficult to measure directly the order parameter discussed in those theories. From a practical standpoint, it will be useful for the verification of theories to observe a change of electronic structure with the HO transition in a visible manner.

Generally, the electronic structure of URu_2Si_2 depends on the duality of $5f$ electrons between itinerant and localized natures. In this regard, the evolution of hybridization between conduction and $5f$ electrons will be responsible for the duality and lead to the change of electronic structure. Additionally, the plural $5f$ electron number will also make its electronic structure more complicated. So far, the electronic structure of HO phase has been investigated by several methods. For example, Aoki *et al.* performed a Shubnikov–de Haas experiment at high fields up to 34 T [8]. They observed all the main branches named α, β, and γ, but there was still a missing Fermi surface (FS) with a large cyclotron mass. On the other hand, Tonegawa *et al.* made a cyclotron resonance experiment in the HO phase and obtained angle-dependent electron masses on the FS sheets [9]. They argued that the κ pocket was corresponding to the missing FS in the quantum oscillation experiment and that the splitting of branch α along the [110] direction was consistent with the nematic state observed by the magnetic torque measurement [10]. Although these results have revealed one aspect of the electronic structure in the HO phase, they have not revealed that of the paramagnetic (PM) phase above T_{HO}. Additionally, such measurements are carried out under high magnetic fields and therefore may observe an excited state. Angle-resolved photoelectron spectroscopy (ARPES) is also an effective method to investigate FSs and band structures. In the HO phase, Boariu *et al.* observed a large hybridization gap opened at the X point in the Brillouin zone (BZ) of a body center tetragonal (BCT) structure [11], while Meng *et al.* found two electron pockets at the equivalent position [12]. In the PM phase, Kawasaki *et al.* reported that no conduction band was observed around the X point [13]. Around the Γ point, a narrow dispersive band has been observed near the Fermi level below T_{HO}. Yoshida *et al.* explained the emergence of a narrow band through the zone folding of a band around the Z point due to the symmetry reduction on the HO transition [14–16]. On the other hand, Chatterjee *et al.* interpreted the narrow band as the formation of the heavy fermion liquid below T_{HO} [17]. These results suggest the contribution of $5f$ electrons to the band structure in the HO phase but with differing findings and explanations. These discrepancies should be partly attributed to the surface sensitivity of ARPES, depending on the energy of the incident beam. In addition, it has been recently pointed out that in spectroscopic experiments with the excitation of f electrons, the resultant images are affected by relaxation energies relevant to the excitation of occupied and empty states [18,19]. Jarlborg *et al.* have shown that in x-ray photoemission spectroscopy, the relaxation energies shift the energy positions of filled f bands by several electron volts below the Fermi energy level E_f, even if the f bands are originally located near E_f [18].

*Corresponding author: akihisa@sci.u-hyogo.ac.jp

Then, in this paper, x-ray Compton scattering was employed as a method to probe the whole picture of how the electronic structure evolves across T_{HO} without being affected by the relaxation energies.

As shown in Eq. (1), the Compton profile, $J(p_z)$ is a one-dimensional projection of electron momentum density (EMD) onto a scattering vector, where EMD is the modulus squared of the momentum space wave function, $\phi(\mathbf{p})$.

$$J(p_z) = \iint |\phi(\mathbf{p})|^2 dp_x dp_y, \tag{1}$$

Therefore, if one wants to obtain the original EMD, the directional Compton profiles are needed to measure a sample of single crystal. Then, the EMD is able to be reconstructed by using the set of Compton profiles. In this paper, we made experiments on the (001) plane in the single crystal of URu_2Si_2 and obtained a two-dimensional (2D) EMD projected on the view plane. Subsequently, the 2D electron occupation number density (EOND) was derived from the EMD through Lock-Crisp-West (LCW) folding analysis [20]. Thanks to the high-energy incident x-ray from a synchrotron radiation source, the 2D EOND exactly reflects the bulk property of electronic structure. The structures in EOND are formed by itinerant bands that pass across E_f, and fully occupied and empty bands make no contribution to the structures [20–22]. Therefore, the change in electronic structure associated with the HO transition is clearly detected, as we see below.

II. EXPERIMENTAL AND ANALYTICAL PROCEDURES

The sample measured was a single crystal grown by using the Czochralski pulling method and was encapsulated in a sealed container for the synchrotron x-ray experiment. The high-resolution Compton profile (HRCP) measurement was made on beamline BL08W at SPring-8. The energy of incident x-ray, ω_1 was 114.56 keV, and the scattering angle was 165.26°. The scattered x-ray was energy resolved by a Si (620) bent crystal analyzer and detected by a position sensitive detector. The energy of the scattered x-ray ω_2 was 79.50 keV at the Compton peak. The difference in energy ω_1-ω_2 is therefore larger than the bound energy of the valence electron. In such a high energy transfer region, Eq. (1) is justified on the basis of impulse approximation [23]. To reconstruct 2D EMD, five directional HRCPs were measured at even intervals between the [100] and [110] crystal axes in the HO (14 K) and PM (20 K) phases. All the HRCPs were carefully corrected for the scattering cross section, background, multiple scattering, and x-ray absorption in the sample. The momentum resolution was 0.11 a.u. Before reconstructing 2D EMD, we subtracted the HRCP at 20 K from that at 14 K to see the change occurring. Figure 1 shows a typical instance of difference profile. Small, but obvious, changes are recognized particularly in low momentum areas, and that ensures the change occurring in the momentum space. For further information, see the Supplemental Material [24].

Respective 2D EMDs above and below T_{HO} were reconstructed by using the set of directional HRCPs. The reconstruction analysis used here was the direct Fourier-transform method [22]. Each directional HRCP was once Fourier transformed into what is called a reciprocal form factor B (r)

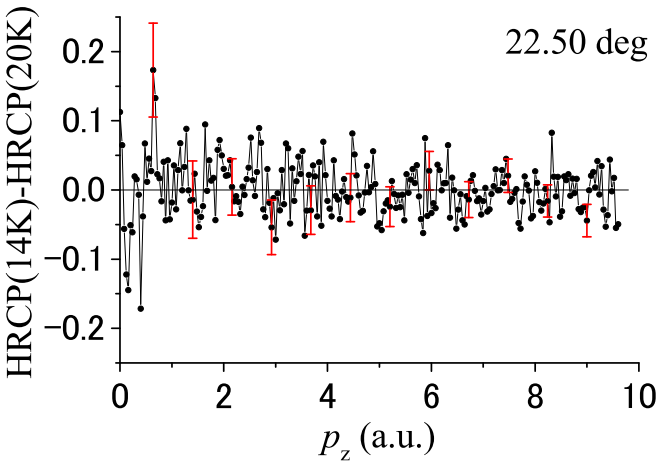

FIG. 1. (Color online) A difference between the two HRCPs measured at 14 and 20 K. The difference profile is taken along the oblique directions of 22.50° from the [100]-axis in the (001) plane. The error bars were estimated from the statistical errors of respective data points in the two HRCPs. For comparison, the error bars in each HRCP are about $1/\sqrt{2}$ size of those in the difference profile.

along that direction. A 2D B (**r**) was obtained by interpolating the plane formed in the set of B (r) functions on a regular grid. The inverse Fourier transform of 2D B (**r**) derived the 2D EMD on the view plane. Here, the 2D EMD was expanded according to the symmetry of crystal. In the case of a many-electron system, the EMD can be expressed in terms of the natural orbitals and therefore described by the corresponding occupation numbers that lie between zero and one [25]. This idea promotes an understanding of the following analysis. Since the EMD is the absolute value of square of momentum space wave functions, the conduction electrons should show a periodic structure in the EMD whenever a position in momentum space is translated with a period of reciprocal lattice vector **G**. Then, the LCW folding was applied to the EMD [20] (see Supplemental Material [24]). This method transforms EMD to EOND in the first BZ by summing the EMD over all **G**s. In the 2D case, its procedure is expressed as

$$n(k_x,k_y) = \sum_{G_x,G_y} \rho(k_x + G_x, k_y + G_y), \tag{2}$$

where n and ρ mean EOND and EMD, respectively. In the present analysis, 21 × 21 BZs were used to derive each 2D EOND, and an average 2D EOND, which includes the contributions from core electrons and fully occupied bands, was subtracted from the original one to emphasize the contribution of conduction electrons to the 2D EOND [26] (see Supplemental Material [24]).

III. RESULTS AND DISCUSSION

Our main finding is how the electronic structure evolves on the HO transition. The electronic structures above and below T_{HO} and its change are clearly reflected in Figs. 2(a)–2(c), respectively, which are the 2D projection of Fermi volumes on the k_x-k_y plane obtained at 14 K ($<T_{HO}$), 20 K ($>T_{HO}$), and the difference between them. Here, the BZ of the BCT structure is adopted. Therefore, the densities at the Γ and Z

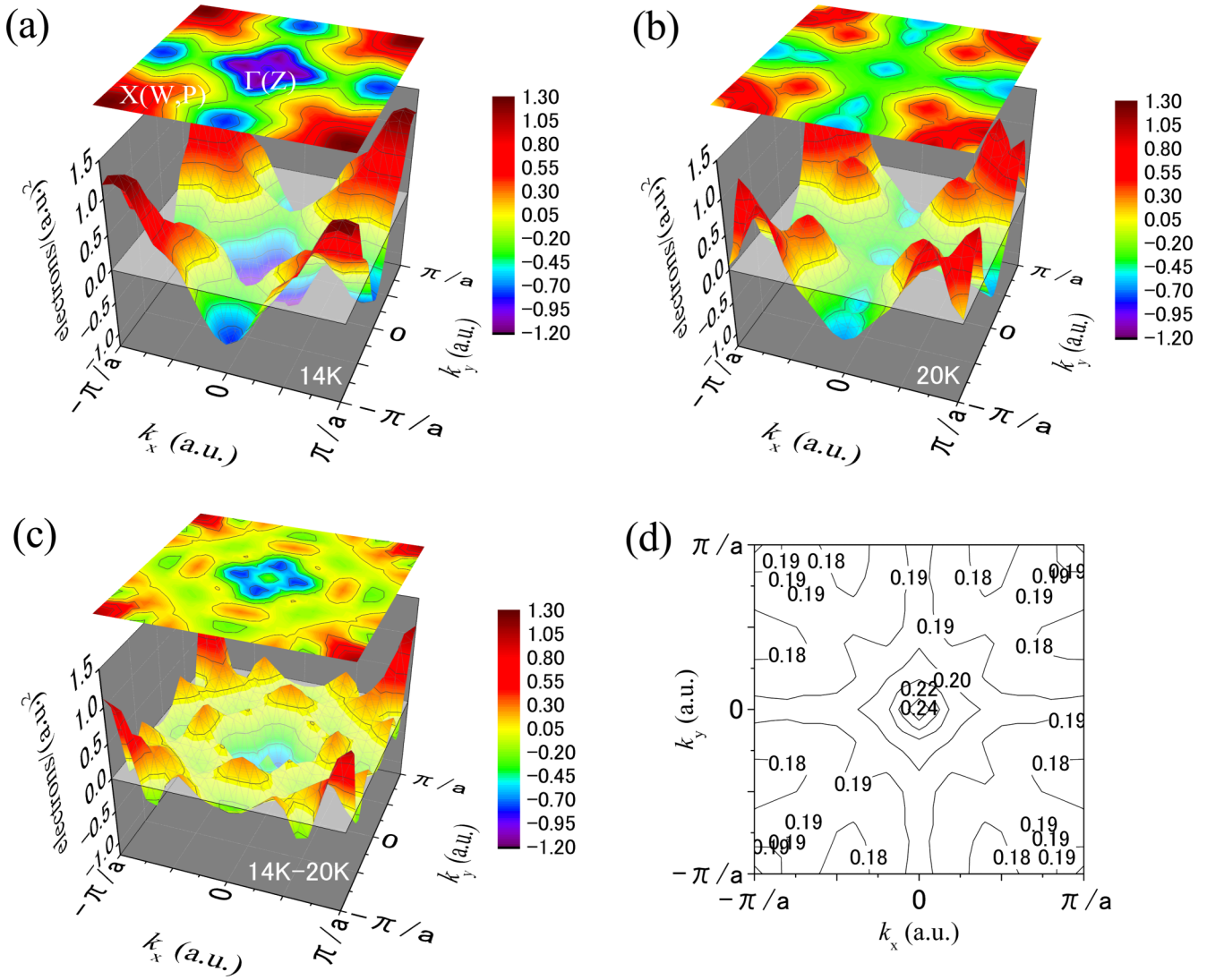

FIG. 2. (Color online) 2D EOND projected on the k_x-k_y plane. (a) The experimental result measured at 14 K. (b) The experimental result measured at 20 K. (c) Difference in 2D EOND between 14 and 20 K. (d) Error distribution of 2D EOND at 20 K. Error distribution at 14 K is mostly the same as that at 20 K. Momentum on the $k_x(k_y)$ axis is indicated in atomic units.

points overlap at the origin, and the structure at the corner of BZ is piled up with the densities along the X, W, and P points. It is apparent that the experimental 2D EOND undergoes drastic changes across T_{HO}, particularly around the origin and the corner of BZ, and shows significant intensities in comparison with the estimated errors in Fig. 2(d). Here, the error propagation was estimated as follows. The experimental errors of each directional HRCP, which were typically $\pm 0.2\%$ around the origin, were put on a simulated profile through the use of random numbers. Then, we made reconstruction and LCW analyses by using the set of simulated profiles with errors. These procedures were repeated until the errors in net result reached convergence. Figure 2(d) is the error map of 2D-EOND at 20 K, and that at 14 K shows most of the same error distribution.

To identify the $5f$ electron contribution to the structures in the 2D EONDs, we have carried out a band calculation within the framework of the local spin density functional approximation. See Supplemental Material [24] for details. Figure 3(a) shows a band structure of URu_2Si_2 derived from the band calculation where all U $5f$ electrons were treated as itinerant ones. This result is consistent basically with the previously reported ones [13,27–29]. It is found from the coloring of each band that the U $5f$ electron component is distributed in the vicinity of E_f. Blue circles in Fig. 3(a) indicate the existence of hole FSs around the Z point in the 17th and 18th bands. Figures 3(b) and 3(c) show the theoretical 2D EONDs due to the projection of the hole Fermi volumes. Red circles in Fig. 3(a) indicate the existence of electron FSs around the Γ and X points in the 19th band, and the theoretical 2D EOND due to the projection of the Fermi volume is shown in Fig. 3(d). Figure 3(e) is the total 2D EOND of those bands. The comparison between Figs. 2 and 3 illustrates that the structure at the corner of BZ in Fig. 2(a) is the projection of electron pocket at the X point and the concave around the origin is attributed to the overlay structure of electron and hole pockets

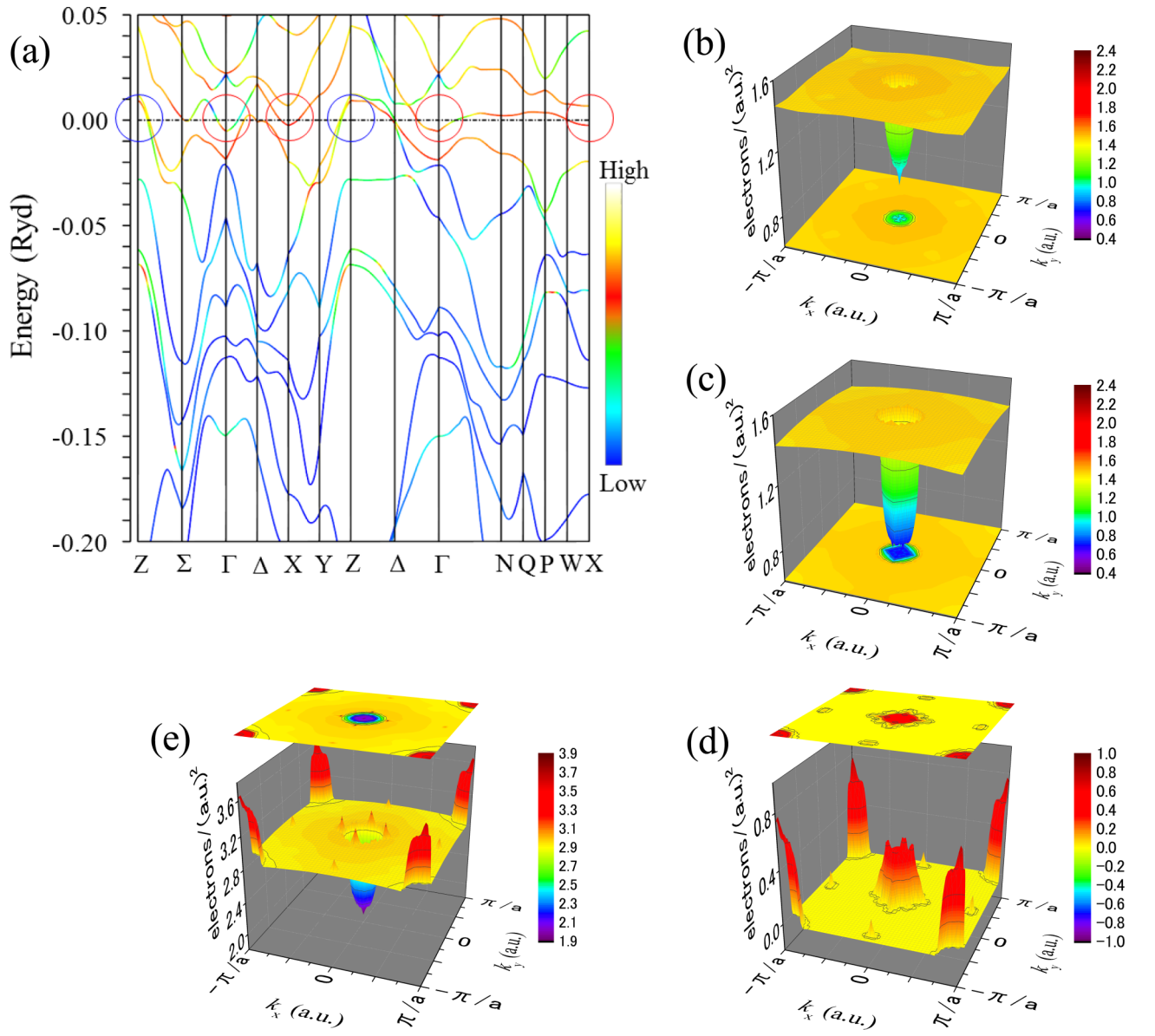

FIG. 3. (Color online) Energy band dispersion and theoretical 2D EONDs. (a) Energy band dispersion calculated with the itinerant 5f electron model. Contribution from U 5f component is indicated on the color scale. Blue and red circles denote the positions of hole and electron FSs. (b)–(d) Theoretical 2D-EONDs of the 17th (b), 18th (c), and 19th (d) bands. (e) Total 2D EOND of those bands.

at the Γ and Z points, respectively. As seen in Fig. 2(b), these structures diminish in the PM phase. In particular, the columnar structure at the corner shrinks, and the concave around the origin shallows. Figure 2(c) reflects the aspect of how the electronic structure changes from the PM to the HO phases and shows a very similar structure to the theoretical EOND in Fig. 3(e). This computation predicates that the 17th, 18th, and 19th bands get deeply involved in the hybridization on the HO transition, resulting in a FS reconstruction around the X, Γ, and Z points.

Since URu_2Si_2 is considered to be a compensated metal, the electron and hole should be the same in number [30]. This aspect allows us to evaluate electron and hole numbers by integrating the absolute value of 2D EOND. The electron (hole) numbers in the HO and PM phases are 0.167 ± 6/f.u. and 0.125 ± 6/f.u., respectively. Therefore, the difference of 0.042/f.u. indicates the change in electron (hole) number associated with the FS reconstruction and will be attributed to 5f electrons, which are densely distributed around the X, Γ, and Z points, as shown in Fig. 3(a). This value is consistent with the hole number evaluated from several Hall effect measurements [30–33], while in that case, the difference in mobility between light hole and heavy electron should be taken into account. On the other hand, the electron (hole) number derived from the present band calculations is 0.190/f.u., which is comparable to the experimental value of the HO phase. In addition, 0.147 out of 0.190 are U 5f electron component in the 19th band.

Here, a comparison of URu_2Si_2 with $CeRu_2Si_2$ provides insight into the meaning of the present results. As a matter of

fact, Figs. 2(a) and 2(b) are very similar to the 2D EONDs of itinerant and localized states in $CeRu_2Si_2$, respectively [26]. In the case of $CeRu_2Si_2$, the change of 2D EONDs is regarded as a gradual crossover phenomenon of a Ce $4f$ electron, while the HO is the second-order phase transition. Note that the 2D EOND in the PM phase appears to be a localized state, although the itinerant nature of $5f$ electrons is considered to evolve in association with the development of Kondo screening below a characteristic temperature $T^*(\sim 50\,\mathrm{K})$ [1–3].

An abrupt change in the 2D EONDs on the HO transition bears out the idea that 0.042 of the $5f$ electrons (holes) retains the localized nature even well below T^* and then turns itinerant through the hybridization in the HO phase, where the 17th-, 18th-, and 19th-like bands come into the picture. In a practical sense, the coherence of $5f$ electrons will not be fully developed in the PM phase above T_{HO}. Since the number of $5f$ electron has been reported to be close to three [34], some of $5f$ electrons are to form fairly flat bands just above T_{HO}, and the incoherent bands should be located very near E_{f}. In fact, recent ARPES experiment has observed incoherent states with no clear dispersion around the Γ point well below T^* [17], even if the relaxation energies shift the energy position. From a comprehensive point of view, 0.042 of the $5f$ electrons (holes) change from incoherent to coherent states through the hybridization and form into the dispersive bands, such as in Fig. 3(a).

As mentioned above, recent theories put the HO transition across clearly and also describe the nematic state [4–7]. However, it does not seem to be easy to examine the validity of theories through the experiment. Since the present results clearly demonstrate the overall electronic structures above and below T_{OH}, it is effective for the verification of theories to determine if each theory can interpret the drastic change of electronic structure. In particular, the description of electronic structure above T_{HO} will be a key to a solution.

IV. SUMMARY

In summary, the whole images of electronic structures above and below T_{HO} are obtained clearly than ever before. The 2D EOND in the HO phase is well described by the band calculation with the itinerant $5f$ electron model, and that in the PM phase reflects the partially localized nature of $5f$ electrons. These results indicate the development of hybridization between the incoherent $5f$ state and the conduction electrons upon crossing T_{HO}. As the result of the hybridization, the 17th-, 18th-, and 19th-like bands will be formed below T_{HO} and contribute to the reconstruction of FSs. The changes in 2D EOND are found not only around the Γ point but also around the X and Z points. Particularly, the change around the X point is a solid finding verified in this paper. Recently, a lattice symmetry breaking at the HO transition has been observed at the zero magnetic field [35]. A tiny difference in lattice constant between two crystal axes will be associated with the electronic nematicity in the HO phase. Thus, the present finding probably signifies the electronic structure of nematic state. The itinerant picture of U $5f$ electron is an appropriate starting point for the description of electronic structure in the HO phase, while the PM phase below T^* should be more complicated state, that is, the coherent and incoherent $5f$ states coexist above T_{HO}.

ACKNOWLEDGMENTS

The synchrotron radiation experiments were performed with the approval of the Japan Synchrotron Radiation Research Institute (JASRI) (Proposals No. 2010B1162 and No. 2011A1499). This paper was supported by Japan Society for the Promotion of Science (JSPS) KAKENHI Grant No. 24540382 and also performed under the Inter-University Cooperative Research Program of the Institute for Materials Research, Tohoku University (Proposal No. 11K0055).

[1] T. T. M. Palstra, A. A. Menovsky, J. van den Berg, A. J. Dirkmaat, P. H. Kes, G. J. Nieuwenhuys, and J. A. Mydosh, Phys. Rev. Lett. **55**, 2727 (1985).

[2] M. B. Maple, J. W. Chen, Y. Dalichaouch, T. Kohara, C. Rossel, M. S. Torikachvili, M. W. McElfresh, and J. D. Thompson, Phys. Rev. Lett. **56**, 185 (1986).

[3] W. Schlabitz, J. Baumann, B. Pollit, U. Rauchschwalbe, H. M. Mayer, U. Ahlheim, and C.D. Bredl, Z. Phys. B **62**, 171 (1986).

[4] C. Pépin, M. R. Norman, S. Burdin, and A. Ferraz, Phys. Rev. Lett. **106**, 106601 (2011).

[5] S. Fujimoto, Phys. Rev. Lett. **106**, 196407 (2011).

[6] H. Ikeda, M. Suzuki, R. Arita, T. Takimoto, T. Shibauchi, and Y. Matsuda, Nat. Phys.**8**, 528 (2012).

[7] P. Chandra, P. Coleman, and R. Flint, Nature (London) **493**, 621 (2013).

[8] D. Aoki, G. Knebel, I. Sheikin, E. Hassinger, L. Malone, T. D. Matsuda, and J. Flouquet, J. Phys. Soc. Jpn. **81**, 074715 (2012).

[9] S. Tonegawa, K. Hashimoto, K. Ikada, Y.-H. Lin, H. Shishido, Y. Haga, T. D. Matsuda, E. Yamamoto, Y. Onuki, H. Ikeda, Y. Matsuda, and T. Shibauchi, Phys. Rev. Lett. **109**, 036401 (2012).

[10] R. Okazaki, T. Shibauchi, H. J. Shi, Y. Haga, T. D. Matsuda, E. Yamamoto, Y. Onuki, H. Ikeda, and Y. Matsuda, Science **331**, 439 (2011).

[11] F. L. Boariu, C. Bareille, H. Schwab, A. Nuber, P. Lejay, T. Durakiewicz, F. Reinert, and A. F. Santander-Syro, Phys. Rev. Lett. **110**, 156404 (2013).

[12] J. Q. Meng, P. M. Oppeneer, J. A. Mydosh, P. S. Riseborough, K. Gofryk, J. J. Joyce, E. D. Bauer, Y. Li, and T. Durakiewicz, Phys. Rev. Lett. **111**, 127002 (2013).

[13] I. Kawasaki, S.-i. Fujimori, Y. Takeda, T. Okane, A. Yasui, Y. Saitoh, H. Yamagami, Y. Haga, E. Yamamoto, and Y. Ōnuki, Phys. Rev. B **83**, 235121 (2011).

[14] R. Yoshida, Y. Nakamura, M. Fukui, Y. Haga, E. Yamamoto, Y. Ōnuki, M. Okawa, S. Shin, M. Hirai, Y. Muraoka, and T. Yokoya, Phys. Rev. B **82**, 205108 (2010).

[15] R. Yoshida, M. Fukui, Y. Haga, E. Yamamoto, Y. Onuki, M. Okawa, W. Malaeb, S. Shin, Y. Muraoka, and T. Yokoya, Phys. Rev. B **85**, 241102(R) (2012).

[16] R. Yoshida, K. Tsubota, T. Ishiga, M. Sunagawa, J. Sonoyama, D. Aoki, J. Flouquet, T. Wakita, Y. Muraoka, and T. Yokoya, Sci. Rep. **3**, 2750 (2013).

[17] S. Chatterjee, J. Trinckauf, T. Hänke, D. E. Shai, J. W. Harter, T. J. Williams, G. M. Luke, K. M. Shen, and J. Geck, Phys. Rev. Lett. **110**, 186401 (2013).
[18] T. Jarlborg, B. Barbiellini, H. Lin, R. S. Markiewicz, and A. Bansil, Phys. Rev. B **84**, 045109 (2011).
[19] T. Jarlborg, B. Barbiellini, C. Lane, Yung Jui Wang, R. S. Markiewicz, Zhi Liu, Zahid Hussain, and A. Bansil, Phys. Rev. B **89**, 165101 (2014).
[20] D. G. Lock, V. H. C. Crisp, and R. N. West, J. Phys. F **3**, 561 (1973).
[21] I. Matsumoto, J. Kwiatkowska, F. Maniawski, M. Itou, H. Kawata, N. Shiotani, S. Kaprzyk, P. E. Mijnarends, B. Barbiellini and A. Bansil, Phys. Rev. B **64**, 045121 (2001).
[22] M. J. Cooper, P. E. Mijnarends, N. Shiotani, N. Sakai, and A. Bansil, *X-ray Compton Scattering* (Oxford University Press Inc., New York, 2004).
[23] I. G. Kaplan, B. Barbiellini, and A. Bansil, Phys. Rev. B **68**, 235104 (2003).
[24] See Supplemental Material at http://link.aps.org/supplemental/10.1103/PhysRevB.92.125112 for detailed descriptions of anisotropy profile, reconstruction of EMD, LCW analysis, and EOND.
[25] Per-Olov Löwdin, Phys. Rev. **97**, 1474 (1955).
[26] A. Koizumi, G. Motoyama, Y. Kubo, T. Tanaka, M. Itou, and Y. Sakurai, Phys. Rev. Lett. **106**, 136401 (2011).
[27] M. Biasini, J. Rusz, and A. P. Mills, Jr., Phys. Rev. B **79**, 085115 (2009).
[28] P. M. Oppeneer, J. Rusz, S. Elgazzar, M.-T. Suzuki, T. Durakiewicz, and J. A. Mydosh, Phys. Rev. B **82**, 205103 (2010).
[29] P. M. Oppeneer, S. Elgazzar, J. Rusz, Q. Feng, T. Durakiewicz, and J. A. Mydosh, Phys. Rev. B **84**, 241102(R) (2011).
[30] Y. Kasahara, T. Iwasawa, H. Shishido, T. Shibauchi, K. Behnia, Y. Haga, T. D. Matsuda, Y. Ōnuki, M. Sigrist, and Y. Matsuda, Phys. Rev. Lett. **99**, 116402 (2007).
[31] J. Schoenes, C. Schönenberger, J. J. M. Franse, and A. A. Menovsky, Phys. Rev. B **35**, 5375 (1987).
[32] R. Bel, H. Jin, K. Behnia, J. Flouquet, and P. Lejay, Phys. Rev. B **70**, 220501(R) (2004).
[33] Y. S. Oh, K. H. Kim, P. A. Sharma, N. Harrison, H. Amitsuka, and J. A. Mydosh, Phys. Rev. Lett. **98**, 016401 (2007).
[34] S. Fujimori, T. Ohkochi, I. Kawasaki, A. Yasui, Y. Takeda, T. Okane, Y. Saitoh, A. Fujimori, H. Yamagami, Y. Haga, E. Yamamoto, Y. Tokiwa, S. Ikeda, T. Sugai, H. Ohkuni, N. Kimura, and Y. Ōnuki, J. Phys. Soc. Jpn. **81**, 014703 (2012).
[35] S. Tonegawa, S. Kasahara, T. Fukuda, K. Sugimoto, N. Yasuda, Y. Tsuruhara, D. Watanabe, Y. Mizukami, Y. Haga, T. D. Matsuda, E. Yamamoto, Y. Onuki, Y. Matsuda, and T. Shibauchi, Nat. Commun. **5**, 4188 (2014).